molecules

MDPI

Article

Ozone Saline Solution Polarizes Microglial Cells Towards an Anti-Inflammatory Phenotype

Federica Armeli [1], Beatrice Mengoni [1], Martina Menin [1], Gregorio Martínez-Sánchez [2], Mauro Martinelli [3], Maurizio Maggiorotti [4] and Rita Businaro [1,*]

[1] Department of Medico-Surgical Sciences and Biotechnologies, Sapienza University of Rome, 04100 Latina, Italy; federica.armeli@uniroma1.it (F.A.); beatrice.mengoni@uniroma1.it (B.M.); menin_martina@yahoo.it (M.M.)
[2] Independent Researcher, 60126 Ancona, Italy; gregorcuba@yahoo.it
[3] Ozone Therapy Unit, Department of Biomedical Sciences, Ospedale San Pietro Fatebenefratelli, 00189 Rome, Italy; mauro.martinelli53@gmail.com
[4] Italian College of Oxygen-Ozone Therapy (CIO3), 00186 Rome, Italy; maggiorotti@gmail.com
* Correspondence: rita.businaro@uniroma1.it

Abstract

Ozone (O_3) therapy has demonstrated antioxidant and anti-inflammatory properties, but the systemic administration of ozonated saline solution (O_3SS) remains underexplored. This study evaluates the cytotoxicity, antioxidant response, and immunomodulatory effects of O_3SS on murine microglial (BV2) and human endothelial (HUVEC) cells. Cells were exposed to increasing doses of O_3 (1, 5, or 10 µg/NmL) dissolved in saline. Viability assays showed that low doses (1 and 5 µg/NmL) enhanced cell proliferation without cytotoxicity, while the highest dose (10 µg/NmL) reduced viability and increased cell death. O_3SS treatment upregulated antioxidant genes, including *Nrf2* and *SOD1*, and decreased reactive oxygen species in lipopolysaccharide (LPS)-stimulated microglia. Additionally, O_3SS modulated microglial phenotype by reducing pro-inflammatory markers (*iNOS*, *IL-1β*) and increasing anti-inflammatory markers (*Arg-1*, *IL-10*). Immunofluorescence confirmed enhanced Arg-1 protein expression, indicating a shift toward an anti-inflammatory state. These results suggest that low-dose O_3SS activates cellular antioxidant defenses and promotes an anti-inflammatory microglial phenotype, supporting its potential as a safe systemic O_3 therapy. Further studies are warranted to confirm in vivo efficacy and optimize clinical protocols.

Keywords: ozone therapy; ozonated saline solution; microglia; anti-inflammatory response; *Nrf2*; reactive oxygen species; cytokines; immunomodulation

check for updates

Academic Editor: George Grant

Received: 25 July 2025
Revised: 12 September 2025
Accepted: 25 September 2025
Published: 30 September 2025

Citation: Armeli, F.; Mengoni, B.; Menin, M.; Martínez-Sánchez, G.; Martinelli, M.; Maggiorotti, M.; Businaro, R. Ozone Saline Solution Polarizes Microglial Cells Towards an Anti-Inflammatory Phenotype. *Molecules* **2025**, *30*, 3932. https://doi.org/10.3390/molecules30193932

Copyright: © 2025 by the authors. Licensee MDPI, Basel, Switzerland. This article is an open access article distributed under the terms and conditions of the Creative Commons Attribution (CC BY) license (https://creativecommons.org/licenses/by/4.0/).

1. Introduction

Ozone (O_3) molecules, formed by three oxygen atoms, are highly unstable. They can quickly break down into one O_2 molecule and one single oxygen atom, which acts as a strong oxidant. O_3 is formed in the atmosphere as a result of electrical discharges and UV light during thunderstorms [1]. In the stratosphere (between 15 and 35 km above sea level), its function is protective, as it shields the Earth from harmful UV rays. In contrast, at the level of the troposphere (10–15 km from the ground), O_3 is produced due to the action of nitrogen oxides and volatile organic pollutants. Together with these pollutants, O_3 causes damage to the respiratory system, predisposing individuals to the development of even

serious pathologies [1]. Due to its strong oxidizing properties, it was widely used during the World Wars for wound treatment and disinfection, and it continues to be

Employed today for water sanitation [2]. The biological effects of O_3 are concentration-dependent and follow a hormetic pattern. While high concentrations (>80 µg/mL) are toxic and harmful, low concentrations within the well-defined therapeutic window (1–80 µg/mL) are beneficial. This beneficial effect is mediated through the stimulation of cellular antioxidant defenses, which are ultimately capable of counteracting oxidative stress, as detailed below [3]. In this context, O_3 has attracted significant interest due to its anti-inflammatory and antioxidant properties, placing it within the scope of complementary medicine—able to support the treatment of certain pathologies without fitting the definition of a pharmaceutical [4]. These characteristics form the basis of O_3 therapy [5–7]. Preclinical studies using in vitro cellular models have elucidated the pathways underlying the protective actions of O_3, and numerous reports have highlighted the therapeutic efficacy of O_3 in pain relief, in the treatment of herniated disks, diabetic foot, osteoarthritis, and various other pathologies of the musculoskeletal system [8]. O_3 is administered in a variety of ways, from topical application for the treatment of skin lesions and oral diseases, to systemic application, for anti-inflammatory and anti-aging, and pro-longevity treatment. For the latter, a mixture of O_3 and oxygen is added to a certain amount of blood taken from the patient and then reinfused back to the patient. This method, although widely used, has several limitations, as it is not always well accepted by patients: it requires large-caliber venous access, and is sometimes refused due to some religious beliefs [9]. It has therefore been proposed to use ozonized saline solution (O_3SS) in which the gas is bubbled and which is then administered to patients via intravenous drip [10].

The aim of this study was to evaluate the cytotoxicity, the antioxidant response, and the immunomodulatory effects of O_3SS on murine microglial cells (BV2) and human endothelial cells (HUVEC). Specifically, we sought to assess the toxic effects of different concentrations of O_3 dissolved in saline and explore the antioxidant and anti-inflammatory responses triggered by O_3 exposure. These effects are of particular interest given the potential use of ozone therapy for treating central nervous system disorders. To address these objectives, we employed two complementary in vitro models. Primary cultures of human endothelial cells were used to evaluate potential cytotoxic effects that may manifest in vivo, specifically as phlebitis. Additionally, a mouse microglial BV2 cell line was utilized to investigate the potential anti-inflammatory as well as antioxidant activity of O_3, given the growing interest in O_3 therapy for neurodegenerative diseases. A key aspect of this study was to determine the minimum effective O_3 concentration that would elicit beneficial antioxidant and anti-inflammatory responses without inducing cytotoxicity. Previous studies have shown that ozone autohemotherapy can provide therapeutic benefits in diseases like acute cerebral infarction [11], with evidence supporting its ability to increase Nrf2 nuclear translocation and the expression of key antioxidants such as SLC7A11 and GPX4 in models of cerebral ischemia/reperfusion injury [12]. Furthermore, ozone therapy has demonstrated its potential in improving the outcomes of central nervous system diseases, particularly in the treatment of ischemic stroke and Alzheimer's disease. O_3 can effectively reduce inflammation, modulate oxidative stress signals, lower amyloid β peptide levels, and improve tissue oxygenation [13]. A further study concluded that Oxygen-O_3 therapy would contribute to improving Multiple Sclerosis (MS) patients by elevating the Treg cell responses [14]. In addition, it is known that the brain microenvironment is shaped by glial cells receiving information from neurons, vascular elements, as well as by peripheral immune signals, providing the rationale for the use of O_3 for the treatment of central nervous system disorders [15]. In this context, our goal was to explore whether O_3 exposure may modulate microglial activation states and stimulate endogenous antioxidant defenses.

Through these models, we aimed to determine whether the O_3SS mixture acts as a modulator of cellular antioxidant pathways and inflammatory responses, thereby supporting its potential use in diseases characterized by oxidative stress and inflammation [16].

2. Results

In the present preclinical study, we aimed to evaluate the efficacy of low doses of O_3SS added to cultures of BV2 microglial cells in carrying out an antioxidant and anti-inflammatory activity, after having evaluated their possible cytotoxic activity.

As shown in Figure 1A, 24 h after O_3 treatment at a concentration of 1 or 5 µg/NmL in saline solution, a significant proliferative response in BV2 cell cultures was detected. On the contrary, the O_3 at a concentration of 10 µg/NmL significantly reduced the number of live cells and increased the number of dead cells. The same doses applied to primary human endothelial cell cultures (HUVECs) are non-cytotoxic and significantly increase the number of viable cells. In contrast, O_3 at concentrations of 5 and 10 µg/NmL leads to an increase in the number of dead cells (Figure 1B).

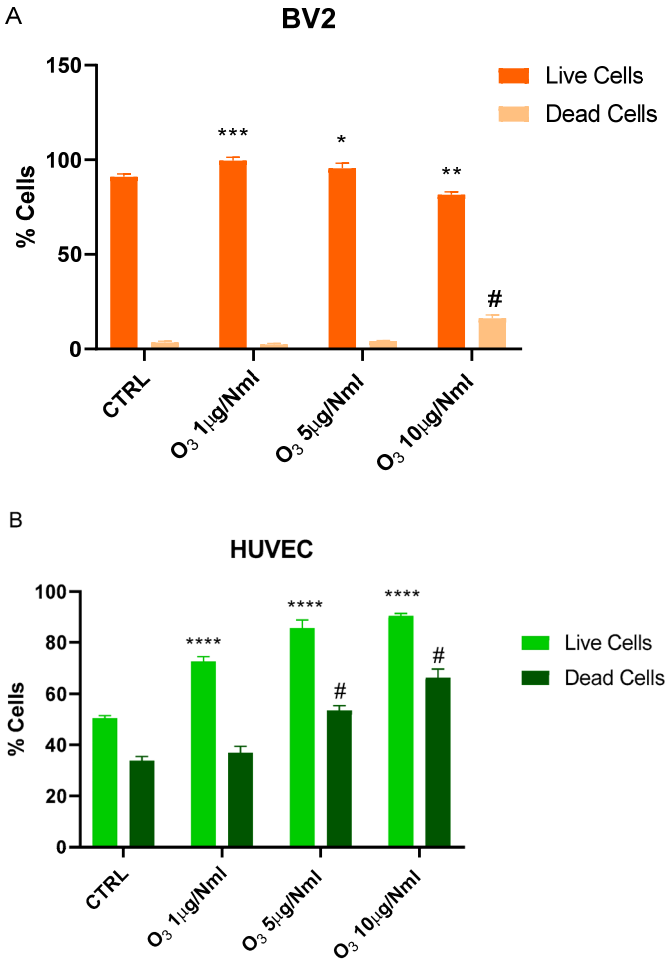

Figure 1. Trypan Blue Assay for O_3 cytotoxicity. (**A**) BV2 cells were treated with 1, 5, or 10 µg/NmL of O_3. (**B**) HUVEC cells were treated with 1, 5, or 10 µg/NmL of O_3. Data are reported as mean ± SD from three independent experiments; statistical analysis was performed using the unpaired Student's *t*-test. * Vs. Live cells; # Vs. Dead cells; * $p < 0.05$; ** $p < 0.01$; *** $p < 0.001$; **** $p < 0.0001$; # $p < 0.05$. CTRL (control).

To rule out that the cytotoxic effects observed in Figure 1 were due to the formation of hypochlorite (ClO^-) during the ozonation process, we measured its concentration in the ozonated solutions using a specific colorimetric kit. The measured hypochlorite

concentration was negligible (0.001%) across all O_3 concentrations tested, a value similar to that found in the culture medium alone and corresponding to the detection limit of the assay kit. This result indicates that hypochlorite formation was not a significant factor contributing to the cytotoxicity of the O_3 solutions.

The activation of cellular antioxidant pathways in response to treatment with O_3 dissolved in 0.9% saline solution was evaluated by the analysis of several mRNAs, respectively, after 4 and 24 h from treatment, as shown in Figure 2. To investigate the molecular mechanism underlying the antioxidant effects of O_3SS, we assessed the activation of the Nrf2 pathway by measuring the expression of Nuclear factor erythroid 2-related factor 2 (*Nrf2*) and Superoxide Dismutase 1 (*SOD1*) mRNA in BV2 cells after 4 or 24 h: after 4 h only the dose of 5 µg/NmL was effective in inducing an increase in *Nrf2* mRNA, while doses of 1 and 10 caused a decrease. The results changed at 24 h where a significant increase in *Nrf2* mRNA expression was observed with both doses of 5 and 10 µg/NmL. *SOD1* mRNA increased both at 4 and 24 h following BV2 treatment with 5 or 10 µg/NmL O_3.

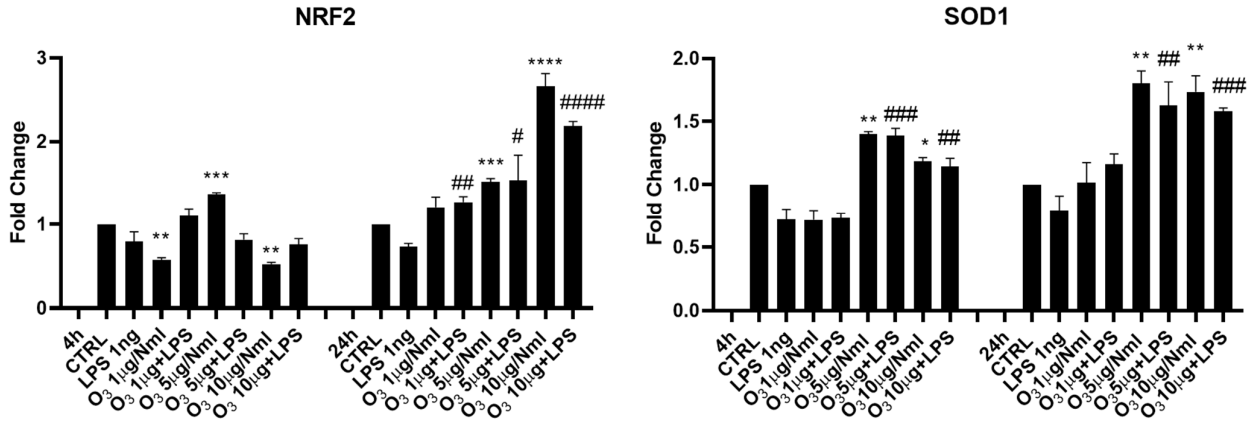

Figure 2. mRNA expression of *Nrf2* and *SOD1* was evaluated by qRT-PCR. Data are shown as mean ± SD from three independent experiments performed in triplicate. Expression profiles were determined using the $2^{-\Delta\Delta CT}$ method. Statistical analysis was reported using unpaired Student's *t*-test. * Vs. CTRL; # Vs. LPS; * $p < 0.05$; ** $p < 0.01$; *** $p < 0.001$; **** $p < 0.0001$; # $p < 0.05$; ## $p < 0.01$; ### $p < 0.001$; #### $p < 0.0001$. CTRL (control) LPS (Lipopolysaccharide).

We then evaluated the expression of Reactive Oxygen Species (ROS) in BV2 microglial cells after treatment with LPS, which is known to induce significant oxidative stress in innate immunity cells, in the presence or absence of O_3. As illustrated in Figure 3, the amount of ROS was decreased in the presence of O_3 treatment in 0.9% saline solution.

We also evaluated the ability of O_3 treatment to reverse the pro-inflammatory phenotype (namely M1 phenotype) induced by the addition of LPS to BV2 microglia cells. We analyzed the expression of mRNAs of *iNOS* (inducible Nitric Oxide Synthase) and *Arg-1* (Arginase-1), two specific markers of the M1 pro-inflammatory phenotype and the M2 anti-inflammatory phenotype, respectively (Figure 4). O_3 at 5 µg/NmL was shown to be able to decrease the expression of *iNOS* mRNA, as measured 4 h after cell treatment; 24 h after treatment, the effective dose was found to be 10 µg/NmL. O_3 administered with saline solution was able to increase the expression of *Arg-1*, a marker of anti-inflammatory polarized microglial cells, at all the tested concentrations, after 4 h from the treatment. In the presence of LPS best results were obtained with 1 and 5 µg/NmL O_3 dissolved in saline solution.

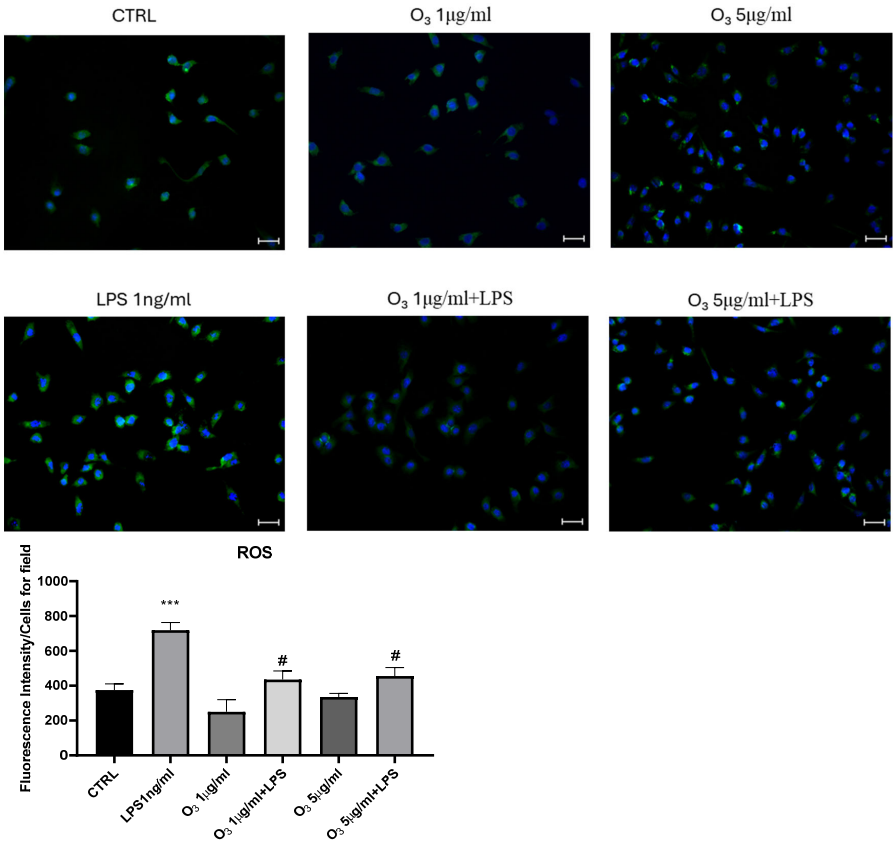

Figure 3. O_3 treatment reduces ROS expression in the LPS-stimulated BV2 cells. Analysis using the cell-permeable probe 2′,7′-dichlorodihydrofluorescein diacetate (H_2DCFDA). Quantification of the median fluorescence of the cell-permeable probe 2′,7′-dichlorodihydrofluorescein diacetate using ImageJ version 1.48. The data are expressed as histograms, normalized to the number of cells in field. 4′,6-diamidino-2-phenylindole (DAPI) was used to counterstain the nuclei. Vs. CTRL *** $p < 0.001$; Vs. LPS # $p < 0.05$; magnification: 20×.

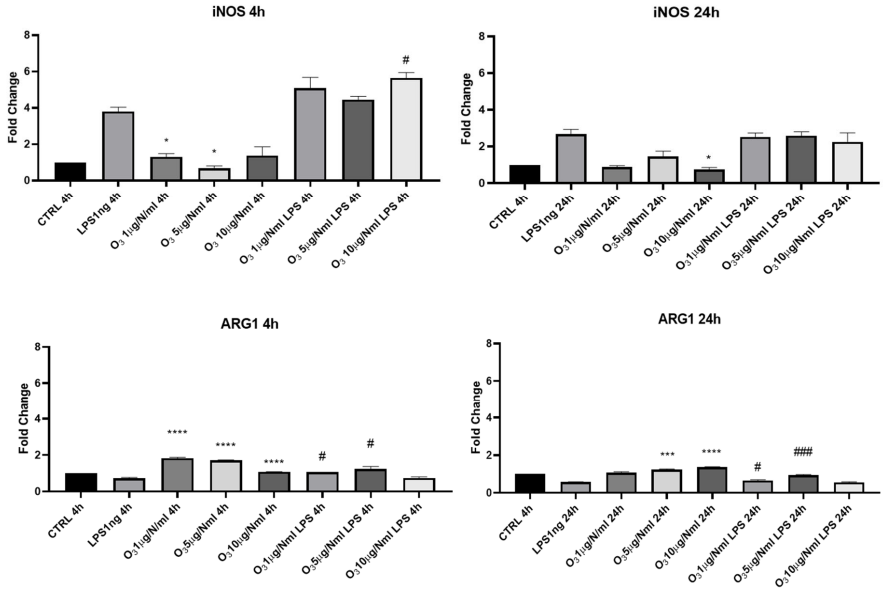

Figure 4. mRNA expression of *iNOS* and *ARG1* was evaluated by qRT-PCR. Data are shown as mean ± SD from three independent experiments performed in triplicate. Expression profiles were determined using the $2^{-\Delta\Delta CT}$ method. Statistical analysis was reported using unpaired Student's *t*-test. * Vs. CTRL; # Vs. LPS; * $p < 0.05$; *** $p < 0.001$; **** $p < 0.0001$; # $p < 0.05$; ### $p < 0.001$.

The anti-inflammatory activity of O_3 treatment was confirmed by immunofluorescence experiments (Figure 5) where O_3SS added at the concentrations of 1 and 5 µg/NmL induced the expression of the protein ARG-1 also in the presence of LPS, counteracting the cell polarization towards a pro-inflammatory phenotype.

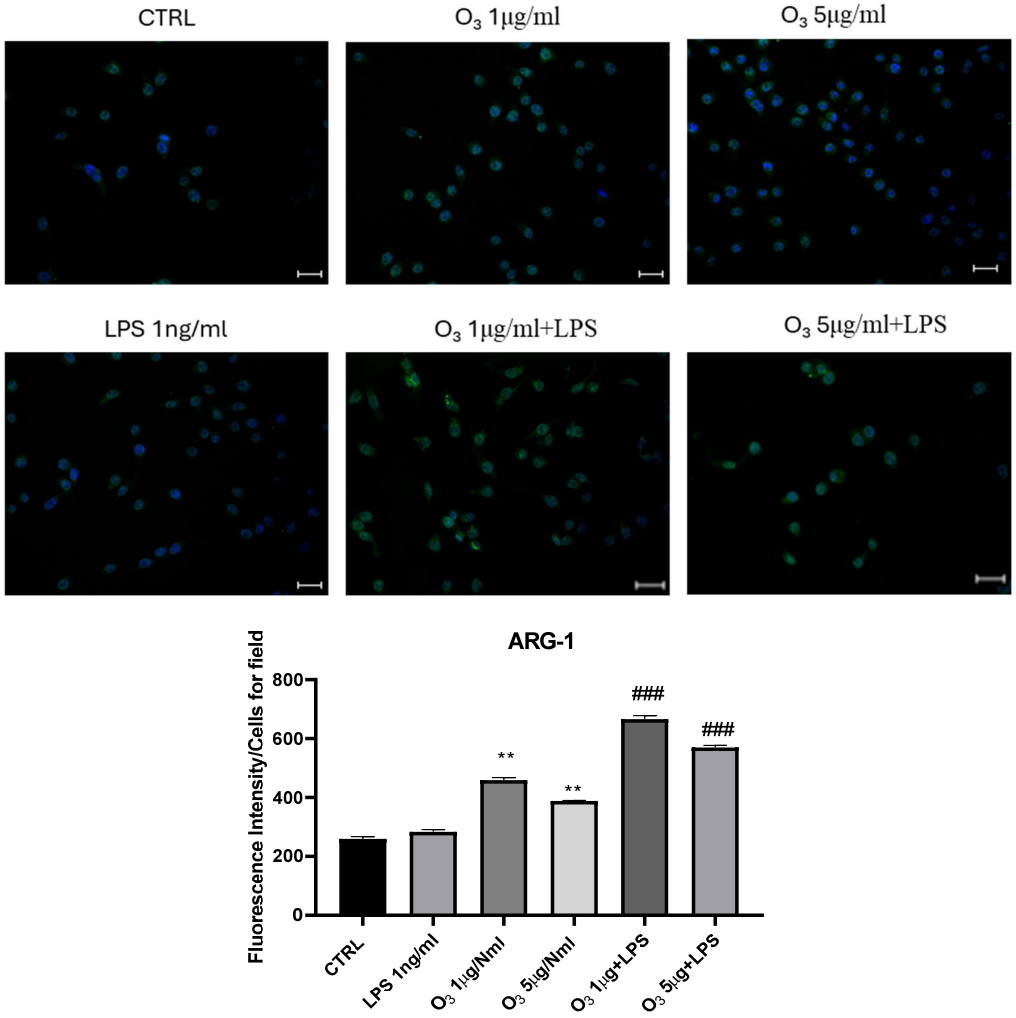

Figure 5. Immunofluorescence analysis of ARG-1 expression in BV2 cells cultured in the presence or absence of LPS for 24 h. Quantification of the median fluorescence intensity was performed by ImageJ software, and data were expressed as histograms, normalized to the number of cells in field. 4′,6-diamidino-2-phenylindole (DAPI) was used to counterstain the nuclei. Data are expressed as mean ± SD for each group (n = 3). Statistical analysis was performed by an unpaired Student's *t*-test. Vs. CTRL ** $p < 0.01$; Vs. LPS ### $p < 0.001$; magnification: 20×.

Furthermore, to confirm the anti-inflammatory activity of O_3SS added to microglial cells, we evaluated the expression of mRNA for the pro-inflammatory cytokine *IL-1β* both in the absence and presence of LPS (Figure 6A). As shown in Figure 6A, O_3 treatment, at all tested concentrations, induced a decrease in *IL-1β* mRNA expression both 4 h and 24 h after treatment. In the presence of LPS, O_3 pretreatment was effective in decreasing *IL-1β* mRNA expression at O_3 concentrations of 5 and 10 µg/NmL; after 24 h from the LPS treatment, all O_3 concentrations were effective in inducing a decrease in *IL-1β* mRNA. We also evaluated the ability of O_3SS to switch microglia cells towards a reparative, anti-inflammatory phenotype (M2) by assessing the expression of the anti-inflammatory cytokine *IL-10* (Figure 6B). O_3 at concentrations of 1, 5, 10 µg/NmL was able to upmodulate the expression of *IL-10* mRNA 4 h after treatment, as shown by RT-PCR experiments. At the same time, it was seen whether this activity was also present after the addition of LPS. After 4 h no significant

variations were appreciated, which instead emerged 24 h after treatment; as a matter of fact, an upmodulation of *IL-10* mRNA was detected both at 1 and 5 µg/NmL O_3, confirming the anti-inflammatory activity of O_3 treatment.

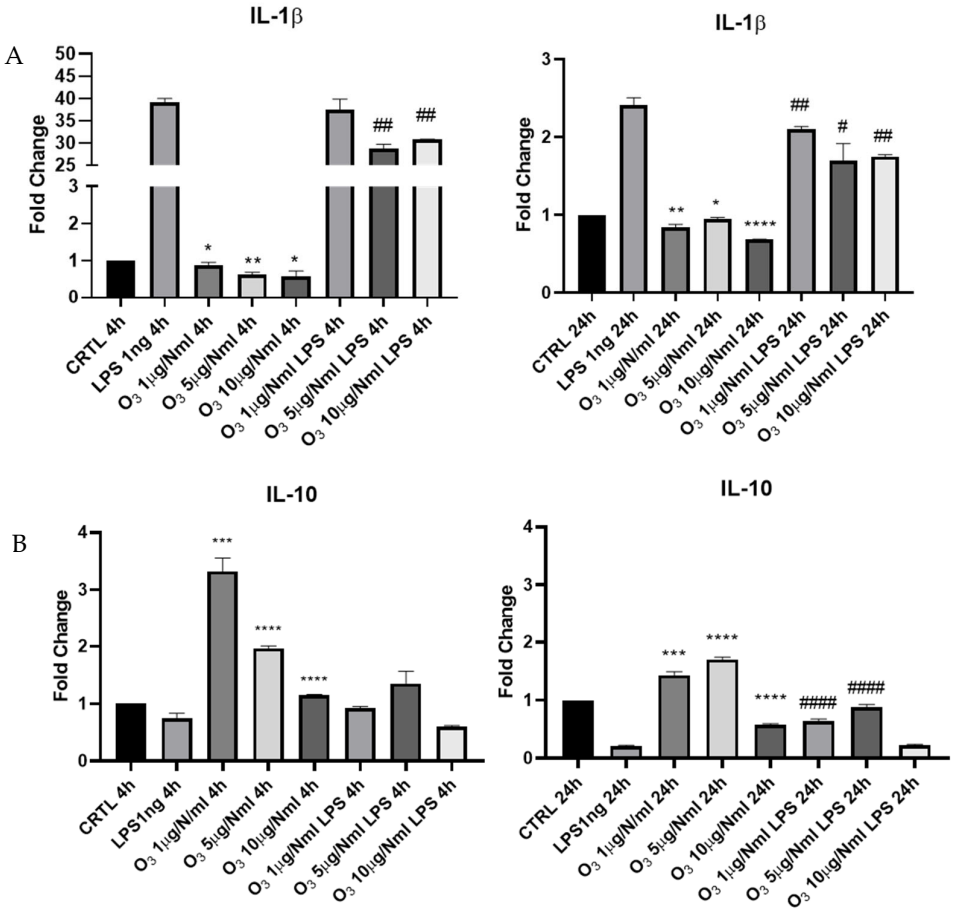

Figure 6. Evaluation of mRNA expression of *IL-1β* (**A**) and *IL-10* (**B**) assessed by qRT-PCR. Data are shown as mean ± SD from three independent experiments performed in triplicate. Expression profiles were determined using the $2^{-\Delta\Delta CT}$ method. Statistical analysis was reported using unpaired Student's *t*-test. Vs. CTRL * $p < 0.05$; ** $p < 0.01$; *** $p < 0.001$; **** $p < 0.0001$; Vs. LPS # $p < 0.05$; ## $p < 0.01$; #### $p < 0.0001$.

3. Discussion

Our study investigated the response of two distinct cellular models—BV2 microglial cells and HUVEC cells—following exposure to O_3-saturated 0.9% saline solution (O_3SS), prepared by bubbling O_3 for 20 min to achieve final concentrations of 1, 5, or 10 µg/NmL. Our results demonstrate that the O_3SS does not present toxic activity in itself in the tested concentration ranges. Previous studies have analyzed the possible reactions taking place after the addition of O_3 to saline solutions, ten ding with cytotoxicity. In this connection, Razumovski et al. (2010) [17] established that O_3 decomposition processes in NaCl aqueous solutions are not accompanied by the formation of noticeable amounts of hypochlorites and chlorates. In addition, Peritiagyn demonstrated that the concentration of sodium hypochlorite in the O_3SS was less than 0.001 g/mL [18]. We have confirmed this result by the hypochlorite detection kit. Moreover, it was demonstrated that ozonation of the saline solution eliminates traces of Bromine that exist in the normal pharmacological formulation of the saline [19]. The kinetics of O_3 saturation in the saline solution were previously studied using spectrophotometric methods. At the concentrations used and with the same medical device and conditions, the O_3 concentration in the solution stabilizes after 10 min

of bubbling and corresponds to 10% of the initial concentration. Under these conditions, the formation of hypochlorous acid or hydrogen peroxide was not detected [20]. Traces of Fe^{2+} in sodium chloride can, in principle, catalyze hydroxyl radical (•OH) generation through the Fenton reaction. However, this requires the presence of H_2O_2 or another suitable peroxide. In pure pharmaceutical-grade NaCl solution (0.9% saline), the European pharmacopeia sets a maximum Fe content of 2 ppm, and under standard ozonation conditions (1–10 µg/mL O_3), no detectable H_2O_2 is formed. Analytical studies confirm H_2O_2 levels remain far below the threshold necessary for Fenton chemistry. Therefore, while Fe^{2+} traces could act as catalysts in theory, in practice under these conditions the formation of hydroxyl radicals via the Fenton reaction is ruled out [21]. The proportion of O_3SS added to the DMEM medium was 1:20. Since DMEM contains a buffering system, significant pH variations after the addition of O_3SS were not expected.

Recently, systemic O_3 application using O_3SS was found to be well tolerated, with no serious adverse events reported in the preliminary study. The intervention, performed under controlled conditions and at low doses (3 µg/NmL), did not result in clinically significant toxicity or hematological abnormalities. Importantly, the study observed a transient increase in the survivor of circulating CD34+ cells following systemic O_3 administration, suggesting a potential stimulatory effect on endothelial–hematopoietic stem/progenitor cell mobilization [22], perhaps explaining the proliferative effect observed on HUVEC cells in our results.

These findings are consistent with the established concept that low-dose O_3 can induce a mild, controlled oxidative eustress, which in turn activates endogenous antioxidant and regenerative pathways without causing cellular damage [23,24]. The observed mobilization of CD34+ cells aligns with the literature describing O_3's capacity to enhance tissue regeneration and modulate immune responses through redox bioregulation [7].

The redox regulatory effect of low doses of O_3 has been repeatedly described and has led to the inclusion of O_3 treatments among the strategies to combat mitochondriopathies linked to high oxidative stress and often due to mitochondrial aging and dysfunction [8]. Several studies demonstrated that the O_3SS-induced response is dependent on the activation of the transduction mechanisms of Nrf2 from cytoplasm to nucleus, inducing antioxidant enzymes synthesis, such as SOD, CAT (catalase), and HO1 (heme oxygenase 1), among others [25–27]. In addition, recent preclinical studies demonstrate that O_3SS mitigates parthanatos after ischemic stroke. In both in vitro (SH-SY5Y cells exposed to H_2O_2) and in vivo (murine ischemic stroke) models, O_3SS administration decreased oxidative stress and neuronal death [28]. Our results confirm the antioxidant activity of O_3SS.

Intravenous infusion of a 5% glucose solution has made it possible to treat patients who could not be treated with the classical method, achieving similar results [29]. However, O_3SS allows for precise control of O_3 dosage and ensures immediate reaction of O_3 with blood components, leading to the formation of redox-active messengers that trigger antioxidant, anti-inflammatory, and immunomodulatory responses. Additionally, O_3SS does not introduce an exogenous glucose load, thereby reducing the risk of metabolic complications such as hyperglycemia or electrolyte disturbances, which are documented risks with intravenous glucose infusions, especially in patients with metabolic comorbidities [30,31]. O_3SS also minimizes the risk of infusion-related complications such as thrombophlebitis, which can occur with repeated glucose infusions [31]. Compared to major autohemotherapy (MAH), which involves ex vivo ozonation of a patient's blood followed by reinfusion, administration of O_3SS offers several practical advantages. O_3SS is technically simpler, avoids direct blood handling, requires a lower caliber needle, and is more acceptable for patients who refuse blood manipulation due to religious or procedural concerns. Additionally, O_3SS generally carries fewer legal implications since it does not

involve extracorporeal blood processing. However, O_3SS has significant disadvantages as a lack of standardization. In general, the medical literature highlights that, while O_3SS may be more convenient in certain settings, MAH remains the preferred method for systemic O_3 therapy due to its superior efficacy, safety, and reproducibility when performed with appropriate protocols and individualized O_3 concentrations. Notwithstanding, clinical evidence supports the efficacy and safety of both MAH and O_3SS infusions in diverse medical contexts. In the study by Makarov et al. (2017) [32], elderly patients undergoing rehabilitation for chronic cardiovascular and musculoskeletal conditions received a combination of MAH or O_3SS and gravitational therapy. Over a follow-up period of up to 7 years, the combination of O_3SS and gravitational therapy resulted in the most significant reduction in the risk of disease progression and need for surgical intervention, as determined by Cox regression analysis. In contrast, a retrospective analysis conducted by Andryushchenko et al. (2019) [33]. A total of 144 patients aged 17 to 72 years (58% women) hospitalized in an intensive care unit in Kyiv received parenteral O_3 therapy as an adjunct to standard care for various acute and chronic conditions, including sepsis, trauma, burns, acute infections, diabetes, and peripheral vascular disease. Two main O_3 therapy modalities were applied: intravenous O_3SS (200 mL containing 0.48 mg of O_3) administered across 169 sessions, or MAH, involving 200–400 mL of autologous blood enriched with 1.8 mg of O_3, across 185 sessions. Clinically, both interventions were associated with improved blood oxygenation, enhanced rheological properties, activation of humoral immunity, and pain relief. Notably, no adverse events or complications were recorded in any of the 304 procedures, underscoring the safety of the approach. The study supports the practical utility of O_3 therapy in emergency medicine and recommends further standardization and controlled clinical trials to validate and refine its use [13,16].

Microglial cells are considered among the main cellular players in the development of neuroinflammation underlying several chronic neurodegenerative diseases, including Alzheimer's disease (AD). For this reason, we chose the BV2 in vitro cellular model, analyzing its behavior after exposure to different amounts of O_3, in the presence or in the absence of LPS. Our results suggest that even with the lowest O_3 concentrations used, microglia are polarized towards an anti-inflammatory phenotype. O_3 is able to downregulate the expression of the pro-inflammatory cytokine *IL-1β*, and the effect is greater after 24 h from treatment, while O_3 alone is able to induce a greater expression of the anti-inflammatory cytokine *IL-10*, increasing its concentration even after exposure to LPS. Furthermore, the cellular markers of pro-inflammatory polarization (*iNOS*) are decreased, while the anti-inflammatory ones (Arg-1) are increased, as detected by real-time PCR and immunofluorescence.

4-hydroxynonenal (4HNE) obtained from Polyunsaturated fatty acids (PUFA) after O_3 addition, increases the expression and transactivation activity of Peroxisome proliferator-activated receptor gamma (PPARγ) [34], and PPARγ was shown to reduce oxidative stress in brain tissue, improving mitochondrial function [35], reducing glial inflammation and Amyloid-beta peptide (Aβ) levels in AD transgenic mouse models [36]. Our data confirm the ability of O_3 to polarize microglial cells towards an anti-inflammatory phenotype, added to cells at low concentrations and dissolved in 0.9% NaCl saline solution. According to the results, 0.9% saline solution exerts a hormetic effect on BV2 microglial cells, characterized by the activation of antioxidant and anti-inflammatory pathways without inducing cytotoxicity at clinically relevant concentrations. The observed upregulation of *Nrf2* and *SOD1* mRNA at 4 and 24 h indicates that O_3 triggers the Keap1/Nrf2-dependent antioxidant response, leading to increased transcription of genes encoding key antioxidant enzymes such as SOD, which is consistent with the established mechanism of low-dose O_3 as a eustress

inducer [37]. This activation enhances the cellular capacity to ROS, as evidenced by the reduction in ROS levels following LPS stimulation.

The modulation of inflammatory markers further supports the immunoregulatory role of O_3. Downregulation of *iNOS* mRNA and upregulation of *Arg-1* mRNA reflect a shift from a pro-inflammatory (M1-like) to an anti-inflammatory (M2-like) microglial phenotype, aligning with the literature showing that low-dose O_3 suppresses pro-inflammatory mediators and promotes anti-inflammatory gene expression [38,39]. This dual action, attenuation of oxidative stress and reprogramming of microglial activation, underpins the therapeutic rationale for O_3 therapy in neuroinflammatory and neurodegenerative contexts.

4. Materials and Methods

4.1. Cell Culture and Treatment

The murine microglial cell line BV-2, kindly provided by Dr. Mangino (Sapienza University of Rome, Italy), was cultured in Dulbecco's Modified Eagle's Medium (DMEM; Sigma-Aldrich, St. Louis, MO, USA) supplemented with 10% fetal bovine serum (FBS; Sigma-Aldrich, St. Louis, MO, USA) and 1% of penicillin–streptomycin, L-glut and non essential amino acids (Sigma-Aldrich, St. Louis, MO, USA), at 37 °C in a humidified atmosphere containing 5% CO_2. Human umbilical vein endothelial cells (HUVECs; Lonza, Basel, Switzerland) were cultured in EGM-2 Endothelial Cell Growth Medium BulletKit (Lonza, Basel, Switzerland) at 37 °C in a 5% CO_2 humidified incubator. Cells were seeded in 6-well plates at a density of 5×10^5 cells/well and incubated at 37 °C.

The human umbilical vein endothelial cells (HUVECs) included in this study were obtained from Lonza (Basel, Switzerland), which collected post-partum umbilical cords with informed consent. As the study did not involve living human subjects and the tissue was obtained as medical waste, Research Ethics Committee approval was not required, in accordance with institutional and national regulations [40–44]. All procedures complied with applicable ethical standards and biosafety guidelines.

The O_3-saline mixture was prepared using the WeZONO device (Deva Med. Sedecal, Madrid, Spain). Treatments were performed by mixing the O_3SS with culture medium at a 1:20 dilution. The ozonized saline was prepared by bubbling an O_2/O_3 gas mixture (output from the WeZONO device (Deva Med. Sedecal, Madrid, Spain)) set at 1, 5, and 10 µg/mL) into 0.9% saline solution (Eurospital, Trieste, Italy) for 20 min. Based on a previously established and validated methodology [20], the actual concentration of O_3 dissolved in the saline solution is 10% of the generator output value, resulting in concentrations of 0.1, 0.5, and 1 µg/mL prior to dilution. O_3 was obtained from clinical-grade oxygen. The accuracy of the O_3 concentration was guaranteed by an internal Algorithm Calculation Measurement system and did not vary by more than 10% of the selected value, in accordance with ISCO3 quality criteria (International Scientific Committee of Ozone Therapy (ISCO3). Guidelines and Recommendations for Medical Professionals Planning to Acquire a Medical Ozone Generator [45] The equipment used is classified within the European Union as a Class IIb medical device.

4.2. Trypan Blue Exclusion Assay

Cell viability was determined by the Trypan-Blue exclusion assay. Trypan-blue (Gibco, Thermo Fisher Scientific, Waltham, MA, USA) exclusion assay is a simple and rapid method measuring cell viability that determines the number of viable cells and dead cells. It is based on the principle that live cells with an intact membrane are able to exclude the dye, whereas dead cells without an intact membrane take up the dye. For the Trypan blue exclusion test, cells were seeded onto 6-well plates at a density of 5×10^5/well. After treatments, cells were detached with 1 × Tripsin-EDTA (Sigma-Aldrich, St. Louis, MO,

USA), and 10 µL of cell suspension was mixed with 10 µL of Trypan Blue solution, and cell counts were performed using a Burker chamber (Paul Marienfeld GmbH & Co. KG, Lauda-Königshofen, Germany). Blue-stained cells were considered nonviable [46].

4.3. Real-Time Quantitative PRC Analysis

Total RNA was extracted from the control and treated cells using the miRNeasy Micro kit (Qiagen, Hilden, Germany) and quantified using NanoDrop One/OneC (Thermo Fisher Scientific, Waltham, MA, USA). cDNA was generated using the High-Capacity cDNA Reverse Transcription kit (Applied Biosystem, Foster City, CA, USA). Quantitative real-time PCR (qPCR) was performed for each sample in triplicate on an Applied Biosystems 7900HT Fast Real-Time PCR System (Applied Biosystem, Cheshire, UK) through the program SDS2.1.1 (Applied Biosystem, Foster City, CA, USA) using the Power SYBR®Green PCR Master Mix (Applied Biosystem, Foster City, CA, USA). The primers for real-time PCR amplification were designed with UCSC GENOME BROWSER (Available online: http://genome.cse.ucsc.edu/ (accessed on 1 November 2022); University of California, Santa Cruz, CA, USA) (Table 1). The primer pair sequences were matched by BLASTn to the genome sequence to identify the primer locations with respect to the exons. A comparative threshold cycle (CT) method was used to analyze the real-time PCR data, where the amount of target, normalized to the endogenous reference of *β-Actin* (ΔCT), and relative to the list of primer couples generated for qRT-PCR.

Table 1. Primers used for real-time PCR amplification.

Gene	Forward Primer (5′–3′)	Reverse Primer (5′–3′)	Accession Numbers
mIL-1β	GAAATGCCACCTTTTGACAGTG	TGGATGCTCTCATCAGGACAG	NM_008361.4
mIL-10	GCCCTTTGCTATGGTGTCCTTTC	TCCCTGGTTTCTCTTCCCAAGAC	NM_010548.2
mARG1	ATGTGCCCTCTGTCTTTTAGGG	GGTCTCTCACGTCATACTCTGT	NM_007482.3
miNOS	GGCAGCCTGTGAGACCTTTG	GCATTGGAAGTGAAGCGTTTC	AF427516.1
mACT-β	GGCTGTATTCCCCTCCATCG	CCAGTTGGTAACAATGCCATGT	NM_007393.5
mNRF2	TCTGAGCCAGGACTACGACG	GAGGTGGTGGTGGTGTCTCTGC	NM_010902
mSOD1	GCCCGCTAAGTGCTGAGTC	AGCCCCAGAAGGATAACGGA	NM_017050

4.4. Immunofluorescence

A total of 30,000 BV2 cells/well of the chamber slides were plated in 200 µL of 10% Fetal Bovine Serum (FBS) in DMEM and stimulated with O_3SS in the presence and absence of lipopolysaccharide (LPS, strain 0111:B4, Sigma-Aldrich, St. Louis, MO, USA) 1 ng/mL for 24 h. After 3 washes in PBS (1x), cells were fixed in 4% paraformaldehyde for 30 min at room temperature. After three washes, cells were permeabilized with 0.1% Triton X-100 for 5 min. Two washes in PBS were performed, and glycine 0.1 M was added for 20 min RT. After two additional washes in PBS, the cells were incubated overnight at 4 °C with the rabbit primary antibody anti-Arginase-1 (AB-84248, Immunological Sciences, Rome, Italy) diluted 1:100 in PBS containing 0.1% BSA [47]. After 3 washes in PBS, the cells were incubated with secondary antibody, goat anti-rabbit IgG (H+L) conjugated with CF488A (Biotium, Fremont, CA, USA, catalog number 20012) for 30 min at room temperature (1:100 in PBS) in the dark. After washing off the excess, the slides were sealed with Vectashield® Antifade Mounting Medium with DAPI (Newark, NJ, USA). Images were acquired and analyzed using NIS-Elements software 4.30.02 (Nikon Instruments Inc., Melville, NY, USA). Using ImageJ software, version 1.48 [48], the fluorescence intensity in the FITC channel was measured for each field and expressed as the mean fluorescence per cell by dividing the total signal by the number of cells measured by DAPI nuclei staining.

4.5. Analysis Using the Cell-Permeable Probe 2′,7′-Dichlorodihydrofluorescein Diacetate (H_2DCFDA)

BV-2 cells were seeded at a density of 50,000 cells per well in chamber slides, in 500 µL of DMEM supplemented with 10% FBS, and subsequently treated with O_3SS. After 45 min, the cells were stimulated with lipopolysaccharide (LPS) at a final concentration of 1 ng/mL and incubated for an additional 4 h at 37 °C. Following the incubation, cells were washed twice with PBS and fixed in 4% paraformaldehyde for 30 min at room temperature. After fixation, two additional PBS washes were performed. Cells were then incubated with the cell-permeable fluorescent probe H_2DCFDA at 37 °C for 30 to 45 min. After staining, cells were washed five times with PBS, then incubated with DAPI (1:100 dilution) for 5 min in the dark. Six final PBS washes were carried out. Finally, coverslips were mounted using Vectashield® Antifade Mounting Medium (Newark, NJ, USA). Images were acquired and analyzed using NIS-Elements software (Nikon Instruments Inc., Melville, NY, USA). Fluorescence intensity was quantified with ImageJ software, version 1.48 [49].

4.6. Detection of Reactive Chlorine Species (Hypochlorous Acid/Hypochlorite)

The measurement of the hypochlorite anion was performed as a crucial control to rule out that the biological effects observed in our experiments were mediated by the potential formation of hypochlorite (ClO^-) as a byproduct of O_3 dissolution, rather than by O_3 itself. To quantify the levels of hypochlorous acid (HClO), we measured the concentration of the hypochlorite anion (ClO^-) using a commercial Hypochlorite Detection Kit (Colorimetric) (ab219929, Abcam, Cambridge, UK). This method is based on a sensor that undergoes a specific reaction with ClO^- to generate a red-colored product, with absorbance measured at 555 nm. Given that HClO dissociates into H^+ and ClO^- (pKa $\approx$ 7.5) and the kit detects the anionic form, the results provide an accurate indirect measurement of the total hypochlorous acid/hypochlorite content in the samples. The assay was performed on the cell culture medium mixed with saline solution at the concentrations previously described, using both HUVEC EBM and DMEM from BV2 cell cultures, and results were compared to the unconditioned culture media used as controls.

4.7. Statistical Analyses

Data were expressed as the mean values ± standard deviations (SD) or mean values ± SEM from at least three independent experiments. Statistical analyses were performed using the unpaired Student's *t* test (GraphPad Prism 8.0.1, San Diego, CA, USA). All results were considered statistically significant with $p < 0.05$. Experiments were performed at least in triplicate.

5. Conclusions

Given these findings, O_3SS may represent a promising adjunctive approach in managing conditions characterized by oxidative stress and inflammation, particularly in cases where MAH is not feasible or is contraindicated. Nonetheless, the current lack of methodological standardization and the absence of robust, large-scale randomized controlled trials highlight the need for further investigation. Future research should prioritize well-designed clinical studies to confirm therapeutic efficacy, optimize dosage regimens, and assess long-term safety. In this study, we explored the effects of systemically administered O_3SS on murine microglial (BV2) and human endothelial (HUVEC) cells, focusing on cytotoxicity, redox regulation, and immunomodulation. Cells were treated with increasing concentrations of O_3 (1, 5, or 10 µg/NmL) dissolved in saline. Low concentrations (1 and 5 µg/NmL) promoted cell proliferation without inducing cytotoxic effects, whereas the highest concentration (10 µg/NmL) led to decreased viability and increased cell death. O_3SS enhanced

the expression of key antioxidant genes such as *Nrf2* and *SOD1*, and significantly reduced reactive oxygen species in LPS-stimulated microglia. Moreover, O_3SS shifted the microglial profile toward an anti-inflammatory phenotype, as evidenced by the downregulation of pro-inflammatory markers (*iNOS*, *IL-1β*) and upregulation of anti-inflammatory mediators (*Arg-1*, *IL-10*), confirmed at the protein level via immunofluorescence. Overall, these results support the potential of low-dose O_3SS to activate endogenous antioxidant defenses and promote immune homeostasis, offering a basis for its further development as a safe and effective systemic O_3 therapy.

6. Limitations

Although our results provide promising evidence of the antioxidant and anti-inflammatory potential of O_3SS, certain limitations must be acknowledged. First, the study was conducted exclusively on cell cultures in vitro (murine microglia BV2 and human endothelial cells HUVEC), which, although informative, do not fully replicate the complexity of physiological environments in vivo. Furthermore, the effects of repeated or chronic exposure to O_3SS were not evaluated, and the short-term cellular responses observed here may not reflect long-term outcomes. Finally, although we observed modulation of antioxidant and inflammatory markers, the molecular mechanisms underlying these effects, such as specific signaling pathways or interactions with redox-sensitive transcription factors, require further investigation. Clinically, O_3 therapy (via O_3SS or MAH) has shown efficacy, without serious adverse effects reported. While both methods have demonstrated safety and potential efficacy, current limitations include variability in O_3 dosing, delivery protocols, and a lack of universal guidelines. Future in vivo studies are essential to validate these findings, determine pharmacokinetics, and establish safe and effective dosing protocols for potential clinical applications.

Author Contributions: Conceptualization, M.M. (Maggiorotti Maurizio), M.M. (Martinelli Mauro), G.M.-S. and R.B.; methodology, F.A., B.M., M.M. (Martinelli Mauro); software, F.A.; investigation, F.A., B.M., M.M. (Menin Martina); resources, R.B.; data curation, F.A.; writing—original draft preparation, F.A. and R.B.; writing—review and editing, G.M.-S. and R.B.; supervision, M.M. (Maggiorotti Maurizio), M.M. (Martinelli Mauro), G.M.-S. and R.B.; project administration, R.B.; funding acquisition, R.B. All authors have read and agreed to the published version of the manuscript.

Funding: This research was funded by Sapienza Ateneo, grant number RM1241910D9FB1F1 to B.R.

Institutional Review Board Statement: Not applicable.

Informed Consent Statement: Not applicable.

Data Availability Statement: The original contributions presented in this study are included in the article.

Conflicts of Interest: The authors declare no conflicts of interest.

References

1. Zhang, J.; Wei, Y.; Fang, Z. Ozone Pollution: A Major Health Hazard Worldwide. *Front. Immunol.* **2019**, *10*, 2518. [CrossRef]
2. Stübinger, S.; Sader, R.; Filippi, A. The Use of Ozone in Dentistry and Maxillofacial Surgery: A Review. *Quintessence Int.* **2006**, *37*, 353–359. [PubMed]
3. Chirumbolo, S.; Tirelli, U.; Franzini, M.; Pandolfi, S.; Ricevuti, G.; Vaiano, F.; Valdenassi, L. Ozone in the Adjunct Medical Treatment. The Round Personality of a Molecule with Hormetic Properties. *Hum. Exp. Toxicol.* **2023**, *42*, 9603271231218926. [CrossRef] [PubMed]
4. Serra, M.E.G.; Baeza-Noci, J.; Mendes Abdala, C.V.; Luvisotto, M.M.; Bertol, C.D.; Anzolin, A.P. The Role of Ozone Treatment as Integrative Medicine. An Evidence and Gap Map. *Front. Public Health* **2023**, *10*, 1112296. [CrossRef]
5. Bocci, V.; Di Paolo, N. Oxygen-Ozone Therapy in Medicine: An Update. *Blood Purif.* **2009**, *28*, 373–376. [CrossRef]

6. Di Mauro, R.; Cantarella, G.; Bernardini, R.; Di Rosa, M.; Barbagallo, I.; Distefano, A.; Longhitano, L.; Vicario, N.; Nicolosi, D.; Lazzarino, G.; et al. The Biochemical and Pharmacological Properties of Ozone: The Smell of Protection in Acute and Chronic Diseases. *Int. J. Mol. Sci.* **2019**, *20*, 634. [CrossRef]
7. Viebahn-Haensler, R.; León Fernández, O.S. Ozone as Redox Bioregulator in Preventive Medicine: The Molecular and Pharmacological Basis of the Low-Dose Ozone Concept—A Review. *Int. J. Mol. Sci.* **2023**, *24*, 15747.
8. Viebahn-Haensler, R.; León Fernández, O.S. Mitochondrial Dysfunction, Its Oxidative Stress-Induced Pathologies and Redox Bioregulation through Low-Dose Medical Ozone: A Systematic Review. *Molecules* **2024**, *29*, 2738. [CrossRef]
9. Masan, J.; Sramka, M.; Rabarova, D. The Possibilities of Using the Effects of Ozone Therapy in Neurology. *Neuro Endocrinol Lett.* **2021**, *42*, 13–21.
10. Schwartz Tapia, A. ISCO3/MET/00/21 Ozonized Saline Solution (O_3SS). ISCO3. 2025. Available online: https://www.google.com/url?q=https://isco3.org/officialdocs/&source=gmail-imap&ust=1759140325000000&usg=AOvVaw0ggJgEAstGR7guKAHarOq5 (accessed on 12 September 2025).
11. Cheng, H.; Lu, R.; Du, J.; Zhao, X.; Zhuang, Z. A Clinical Study on Ozone Autohemotherapy for the Treatment of Acute Ischemic Stroke. *Front. Med.* **2025**, *12*, 1595568. [CrossRef]
12. Zhu, F.; Ding, S.; Liu, Y.; Wang, X.; Wu, Z. Ozone-Mediated Cerebral Protection: Unraveling the Mechanism through Ferroptosis and the NRF2/SLC7A11/GPX4 Signaling Pathway. *J. Chem. Neuroanat.* **2024**, *136*, 102387. [CrossRef] [PubMed]
13. Zhang, X.; Wang, S.-J.; Wan, S.-C.; Li, X.; Chen, G. Ozone: Complicated Effects in Central Nervous System Diseases. *Med. Gas Res.* **2025**, *15*, 44–57. [CrossRef] [PubMed]
14. Tahmasebi, S.; Qasim, M.T.; Krivenkova, M.V.; Zekiy, A.O.; Thangavelu, L.; Aravindhan, S.; Izadi, M.; Jadidi-Niaragh, F.; Ghaebi, M.; Aslani, S.; et al. The Effects of Oxygen–Ozone Therapy on Regulatory T-cell Responses in Multiple Sclerosis Patients. *Cell Biol. Int.* **2021**, *45*, 1498–1509. [CrossRef] [PubMed]
15. Müller, L.; Di Benedetto, S.; Müller, V. The Dual Nature of Neuroinflammation in Networked Brain. *Front. Immunol.* **2025**, *16*, 1659947. [CrossRef]
16. Yin, F.; Sancheti, H.; Patil, I.; Cadenas, E. Energy Metabolism and Inflammation in Brain Aging and Alzheimer's Disease. *Free. Radic. Biol. Med.* **2016**, *100*, 108–122. [CrossRef]
17. Razumovskii, S.D.; Konstantinova, M.L.; Grinevich, T.V.; Korovina, G.V.; Zaitsev, V.Y. Mechanism and Kinetics of the Reaction of Ozone with Sodium Chloride in Aqueous Solutions. *Kinet. Catal* **2010**, *51*, 492–496. [CrossRef]
18. Peretiagin, S.P.; Struchkov, A.A.; Peretiagin, N.C.; Kulechina, N.B. Ozonization Method of Saline Solution. Russian Patent RU2289413. 10 February 2006. Available online: https://patentimages.storage.googleapis.com/b4/e7/c6/6a593e156466b9/RU2289413C2.pdf (accessed on 29 September 2025).
19. Ma, L.; Wen, S.; Yuan, J.; Zhang, D.; Lu, Y.; Zhang, Y.; Li, Y.; Cao, S. Detection of Chlorite, Chlorate and Perchlorate in Ozonated Saline. *Exp. Ther. Med.* **2020**, *20*, 2569–2576. [CrossRef]
20. Sánchez, G.M. Practical Aspects in Ozone Therapy: Study of the Ozone Concentration in the Ozonized Saline Solution. *Ozone Ther. Glob. J.* **2020**, *10*, 56–68.
21. De Vera, G.A.; Stalter, D.; Gernjak, W.; Weinberg, H.S.; Keller, J.; Farré, M.J. Towards Reducing DBP Formation Potential of Drinking Water by Favouring Direct Ozone over Hydroxyl Radical Reactions during Ozonation. *Water Res.* **2015**, *87*, 49–58. [CrossRef]
22. Cachay Agurto, J.U.; Huambo-Chávez, J.A.; Vásquez-Bravo, M.; Álvarez Ángeles, M.A.; Angulo Cornejo, H.H.; Garcia Terzo, L.; Martínez-Sánchez, G. Systemic Ozone Application and Its Impact on the Mobilization of CD34+ Cells. Preliminary Study. *G. Ital. Ozono Ter. House Organ Nuova FIO* **2024**, *18*, 9–15.
23. Malatesta, M.; Tabaracci, G.; Pellicciari, C. Low-Dose Ozone as a Eustress Inducer: Experimental Evidence of the Molecular Mechanisms Accounting for Its Therapeutic Action. *Int. J. Mol. Sci.* **2024**, *25*, 12657. [CrossRef]
24. Tricarico, G.; Travagli, V. The Relationship between Ozone and Human Blood in the Course of a Well-Controlled, Mild, and Transitory Oxidative Eustress. *Antioxidants* **2021**, *10*, 1946. [CrossRef] [PubMed]
25. Kim, M.Y.; Song, K.S.; Park, G.H.; Chang, S.H.; Kim, H.W.; Park, J.H.; Jin, H.; Eu, K.J.; Cho, H.S.; Kang, G.; et al. B6C3F1 Mice Exposed to Ozone with 4-(N-Methyl-N-Nitrosamino)-1-(3-Pyridyl)-1-Butanone and/or Dibutyl Phthalate Showed Toxicities through Alterations of NF-kappaB, AP-1, Nrf2, and Osteopontin. *J. Vet. Sci.* **2004**, *5*, 131–137. [CrossRef] [PubMed]
26. Cho, H.-Y.; Gladwell, W.; Yamamoto, M.; Kleeberger, S.R. Exacerbated Airway Toxicity of Environmental Oxidant Ozone in Mice Deficient in *Nrf2*. *Oxidative Med. Cell. Longev.* **2013**, *2013*, 254069. [CrossRef] [PubMed]
27. Qu, D.; Peng, F.; Liu, L.; Yang, S.; Guo, Y. Effect of ozonized saline on signaling passway of Keap1-Nrf2-ARE in rat hepatocytes. *Zhonghua Gan Zang Bing Za Zhi* **2011**, *19*, 367–371. [CrossRef]
28. Li, J.; Liu, X.; Wang, Z.; Xie, P.; Zhu, M.; Zhong, H.; Luo, S.; Tang, J.; Mo, G. Ozone Therapy Mitigates Parthanatos after Ischemic Stroke. *Biol. Res.* **2024**, *57*, 1–14. [CrossRef]
29. Martinelli, M.; Romanello, D. Systemic Ozone Therapy May Improve the Perception of Quality of Life: Ozonized Glucose Solution 5% Extends Reach to Patients Ineligible for Blood Infusion. *Cureus* **2024**, *16*, e64629. [CrossRef]

30. Tellan, G.; Iannarone, C.; Fegiz, A.; Baumgartner, I.; Maselli, A.M.; Fantera, A. Variation of Acid-Base Balance, Glycemia, Electrolytes and ETCO2 after Fast i.v. Infusion of 5% Fructose and/or Glucose. *Eur. Rev. Med. Pharmacol. Sci.* **1997**, *1*, 161–165.
31. Hessov, I.; Bojsen-Møller, M.; Melsen, F. Experimental Infusion Thrombophlebitis: A Comparison between Glucose and Fructose and 5% and 10% Glucose Solutions. *Intensive Care Med.* **1979**, *5*, 79–81. [CrossRef]
32. Makarov, I.V.; Shchukin, Y.V.; Lukashova, A.V. Effect of combined application of ozone therapy and gravitational therapy on the remote results of complex treatment of geriatric patients. *Adv. Gerontol.* **2017**, *30*, 558–562.
33. Andryushchenko, V.V. Current Issues of Practical Application of Parenteral Ozone Therapy in Emergency Medicine. *Emerg. Med.* **2019**, *8*, 121–127. [CrossRef]
34. Wang, Z.; Dou, X.; Gu, D.; Shen, C.; Yao, T.; Nguyen, V.; Braunschweig, C.; Song, Z. 4-Hydroxynonenal Differentially Regulates Adiponectin Gene Expression and Secretion via Activating PPARγ and Accelerating Ubiquitin–Proteasome Degradation. *Mol. Cell. Endocrinol.* **2012**, *349*, 222–231. [CrossRef] [PubMed]
35. Marion-Letellier, R.; Savoye, G.; Ghosh, S. Fatty Acids, Eicosanoids and PPAR Gamma. *Eur. J. Pharmacol.* **2016**, *785*, 44–49. [CrossRef] [PubMed]
36. Dhapola, R.; Hota, S.S.; Sarma, P.; Bhattacharyya, A.; Medhi, B.; Reddy, D.H. Recent Advances in Molecular Pathways and Therapeutic Implications Targeting Neuroinflammation for Alzheimer's Disease. *Inflammopharmacology* **2021**, *29*, 1669–1681. [CrossRef]
37. Galiè, M.; Costanzo, M.; Nodari, A.; Boschi, F.; Calderan, L.; Mannucci, S.; Covi, V.; Tabaracci, G.; Malatesta, M. Mild Ozonisation Activates Antioxidant Cell Response by the Keap1/Nrf2 Dependent Pathway. *Free. Radic. Biol. Med.* **2018**, *124*, 114–121. [CrossRef]
38. Lacavalla, M.A.; Inguscio, C.R.; Cisterna, B.; Bernardi, P.; Costanzo, M.; Galiè, M.; Scambi, I.; Angelini, O.; Tabaracci, G.; Malatesta, M. Ozone at Low Concentration Modulates Microglial Activity in Vitro: A Multimodal Microscopy and Biomolecular Study. *Microsc. Res. Tech.* **2022**, *85*, 3777–3792. [CrossRef]
39. Cenci, A.; Macchia, I.; La Sorsa, V.; Sbarigia, C.; Di Donna, V.; Pietraforte, D. Mechanisms of Action of Ozone Therapy in Emerging Viral Diseases: Immunomodulatory Effects and Therapeutic Advantages With Reference to SARS-CoV-2. *Front. Microbiol.* **2022**, *13*, 871645. [CrossRef]
40. Chandel, S.; Kumaragurubaran, R.; Giri, H.; Dixit, M. Isolation and Culture of Human Umbilical Vein Endothelial Cells (HUVECs). In *Vascular Hyperpermeability*; Tharakan, B., Ed.; Methods in Molecular Biology; Springer: New York, NY, USA, 2024; Volume 2711, pp. 147–162. ISBN 978-1-07-163428-8.
41. Siow, R.C.M. Culture of Human Endothelial Cells from Umbilical Veins. In *Human Cell Culture Protocols*; Mitry, R.R., Hughes, R.D., Eds.; Methods in Molecular Biology; Humana Press: Totowa, NJ, USA, 2012; Volume 806, pp. 265–274. ISBN 978-1-61779-366-0.
42. Jiménez, N.; Krouwer, V.J.D.; Post, J.A. A New, Rapid and Reproducible Method to Obtain High Quality Endothelium in Vitro. *Cytotechnology* **2013**, *65*, 1–14. [CrossRef]
43. Lei, J.; Peng, S.; Samuel, S.B.; Zhang, S.; Wu, Y.; Wang, P.; Li, Y.-F.; Liu, H. A Simple and Biosafe Method for Isolation of Human Umbilical Vein Endothelial Cells. *Anal. Biochem.* **2016**, *508*, 15–18. [CrossRef]
44. Śladowski, D.; Combes, R.; Van Der Valk, J.; Nawrot, I.; Gut, G. ESTIV Questionnaire on the Acquisition and Use of Primary Human Cells and Tissue in Toxicology. *Toxicol. Vitr.* **2005**, *19*, 1009–1013. [CrossRef]
45. ISCO3. 2019. Available online: https://isco3.org/wp-content/uploads/2015/09/Generadores-ISCO3-SOP-DEV-01-01-2019.pdf (accessed on 12 September 2025).
46. Louis, K.S.; Siegel, A.C. Cell Viability Analysis Using Trypan Blue: Manual and Automated Methods. *Methods Mol. Biol.* **2011**, *740*, 7–12. [CrossRef]
47. Luan, W.; Li, M.; Wu, C.; Shen, X.; Sun, Z. Proteomic Dissimilarities of Primary Microglia and BV2 Cells under Stimuli. *Eur. J. Neurosci.* **2022**, *55*, 1709–1723. [CrossRef]
48. Schneider, C.A.; Rasband, W.S.; Eliceiri, K.W. NIH Image to ImageJ: 25 Years of Image Analysis. *Nat. Methods* **2012**, *9*, 671–675. [CrossRef]
49. Rak, M.; Reiss, K. Double Labeling Fluorescent Immunocytochemistry. In *Methods in Molecular Biology*; Springer: New York, NY, USA, 2022; pp. 147–161. ISBN 978-1-07-161947-6.

Disclaimer/Publisher's Note: The statements, opinions and data contained in all publications are solely those of the individual author(s) and contributor(s) and not of MDPI and/or the editor(s). MDPI and/or the editor(s) disclaim responsibility for any injury to people or property resulting from any ideas, methods, instructions or products referred to in the content.